Mecánica Computacional Vol. XXI, pp. 1461–1470
S. R. Idelsohn, V. E. Sonzogni and A. Cardona (Eds.)
Santa Fe–Paraná, Argentina, October 2002

A MESHLESS METHOD FOR KIRCHOFF PLATE MODEL

Enrique Pardo and Octavio Pagano

Facultad de Ingeniería
Universidad de Mar del Plata, Argentina
e-mail: epardo@fi.mdp.edu.ar

Key words: Kirchhoff thin plate theory, meshless methods

Abstract. *In this work we describe and analyze the application of a meshless method to static and dynamic calculation of Kirchhoff thin plate problems. The method is based on the use of blurred derivatives. Briefly, blurred derivatives allow to transform differential equations into an integral equation which does no contain derivatives of the unknown function. The final expression is an updating formula which only has physical meaning in a limit known as a functional integral, so that the technique is designated as the Functional Integral Formulation (FIM) of continuous problems.*

The application of this meshless method for modeling plate problems offers a number of advantages over the traditional finite element method. It considerably simplifies data preparation in highly irregular structures and allows to use "p-refinement" without modifying the net of nodes.

In this work we first describe the basics of the method and its computational implementation. The method is the applied to a static problem comparing its performance with rectangular finite elements. Finally, its feasibility for calculation of free vibrations of plates is demonstrated.

1 INTRODUCTION

During the last decade a number of meshless methods have been designed to overcome the difficulties posed by the generation of meshes (i.e. partitions of the domain) in three dimensional problems. Some of the methods developed so far are the Diffuse Element Method[1] and the Element Free Galerkin Method[2] (which use MLS interpolation), hp-Clouds[3], Smooth Particle Hydrodynamics[4], Reproducing Kernel Particle Methods[5],Natural Element Method[6], Generalized Finite Differences[7], etc. However, the use of such methods in the framework of approximate theories, such as beams, plates and shells has began only very recently. For example, the hp-Cloud Method has been successfully applied to Timoshenko beam problems by Barcellos *et. al*.[8] and to Mindlin's plates by García *et. al*.[9] Also, boundary integrals with moving least-squares approximations were used to model Kircchoff thin plates by Sladek *et. al*.[10]

In this work we present the use of the Functional Integral Formulation[11-13] to solve Kirchoff thin plate problems. First, the governing differential equation is transformed into an integral updating formula that lead very naturally for meshless computational implementations. This is followed by a discussion on discretization using simple polynomials and boundary conditions enforcement. Finally, numerical examples of statics and dynamics are analyzed and compared with finite elements. It is shown that the present method allows better accuracy and higher convergence rates than the latter.

2.- KIRCHHOFF THIN PLATE EQUATIONS

Thin plates are plane structures with one of its dimensions, the thickness, much smaller than the in-plane dimensions. This allows to make some simplifying assumptions in order to avoid a full three dimensional modeling of the structure. The two most important assumptions are:

a) Sections normal to the middle plane remain plane after deformation
b) Stresses normal to the plate surface are negligible

If the thickness, h, is small enough (i.e. smaller that 1/10 of the smallest in-plane dimension) a third hypothesis can be added (Bernoulli-Euler assumption)

c) Shear deformation is negligible

The three above mentioned restrictions define the Kirchhoff thin plate model. In this simplified mathematical model there is a single independent variable which is the displacement normal to the plate surface (lying on the x,y plane), W(x,y). The other two displacements are related to the former by:

$$u(x,y,z) = -\theta_x(x,y).z \quad ; \quad \theta_x = \frac{\partial W}{\partial x}$$
$$v(x,y,z) = -\theta_y(x,y).z \quad ; \quad \theta_y = \frac{\partial W}{\partial y} \qquad (1)$$

, and the traverse displacement satisfies the well known fourth order differential equation:

$$D\nabla^2\nabla^2 W + \rho h \frac{\partial^2 W}{\partial t^2} = p(x, y) \tag{2}$$

Where D is the plate stiffness, ρ is density and p is the pressure on the plate surface.
The problem can be stated in weak form either by application of the virtual work principle or Galerkin weighted residuals to equation (2). The resulting statement contains second derivatives of the displacement W, so that C^1 continuity of shape functions is required. This stringent limitation have fueled research on plate and shell finite elements during the past two decades. A large number of elements of varying complexity is available, as reviewed in many textbooks.
Recently, some meshless methods of solution have been applied to this problem. , which do not require inter-element

3 MESHLESS METHOD BASE ON BLURRED DERIVATIVES

Blurred derivatives stem from a very simple observation: the value of a continuous function at a point can be evaluated as:

$$f_{(x,y)} = \lim_{\delta \to 0} \int_{-\infty}^{\infty} P^0_{(\bar{\mathbf{r}}-\mathbf{r},\delta)} \cdot f_{(\bar{\mathbf{r}})} . d\overline{V} \tag{3}$$

Where $\bar{\mathbf{r}} = (\bar{x}, \bar{y})^t$; $\mathbf{r} = (x, y)^t$; $d\overline{V} = d\bar{x}.d\bar{y}$

The operator P^0 of (3) is the zero order blurred derivative kernel:

$$P^0_{(\bar{\mathbf{r}}-\mathbf{r},\delta)} = \frac{e^{-\frac{(\bar{\mathbf{r}}-\mathbf{r})^2}{\delta^2}}}{\pi.\delta^2} \tag{4}$$

Derivatives of the function $f_{(x,y)}$ in (3) can be evaluated by differentiation of the zero order kernel. A comprehensive study of blurred derivatives and its application to numerical solution of differential equations can be found elsewhere. For our purposes it suffices to define the

blurred derivative kernel corresponding to the biharmonic operator of equation (2), which is found to be:

$$P^4 = \nabla^2\nabla^2 P^0 = \frac{16}{\delta^4} P^0\left[\left(2 - r'^2\right)^2 - 2\right] \tag{5}$$

Where $\mathbf{r}' = \frac{\mathbf{r}}{\delta}$

Notice that a given zero order kernel generates an associated set of kernels by differentiation. In particular, within the Gaussian family the zero order kernel given by formula (4) generates the first set. The second generation starts with a zero order kernel similar to (4) multiplied by a second degree polynomial. The third generation starts with the zero order kernel:

$${}^2P^0_{(\bar{\mathbf{r}}-\mathbf{r},\delta)} = \frac{e^{-\frac{(\bar{\mathbf{r}}-\mathbf{r})^2}{\delta^2}}}{\pi.\delta^2}\left[3 - 3r'^2 + \frac{1}{2}r'^4\right] \tag{6}$$

The kernels (5) and (6) satisfy the relation

$${}^2P^0 - \frac{\delta^4}{32}P^4 = P^0\left[2 - r'^2\right] \equiv P_{(\mathbf{r}'-\mathbf{r},\delta)} \tag{7}$$

This relation will be used in the derivation of a numerical scheme below.

5.- Approximation of the differential equation

To obtain a numerical scheme for solving equation (2) using blurred derivatives, it must be first transformed into an updating prescription for the field W(x,y). To this end we first approximate the time derivative of W using finite differences:

$$\frac{\partial^2 W}{\partial t^2} \cong \frac{\dot{W}(x,y,t+\varepsilon) - \dot{W}(x,y,t)}{\varepsilon} \tag{8}$$

Where the dot designates the first time derivative and ε is a sufficiently small time step. Equation (2) is the approximated as:

$$\dot{W}(x,y,t+\varepsilon) \cong -\varepsilon\kappa\nabla^2\nabla^2 W + \varepsilon p'(x,y) + \dot{W}(x,y,t) \tag{9}$$

Where we abbreviated: $\kappa = \frac{D}{\rho h}$; $p' = \frac{p}{\rho h}$. Replacing the right member of (9) by a finite difference approximation we have:

$$W(x,y,t+\varepsilon) \cong W(x,y,t) - \varepsilon^2 \kappa \nabla^2 \nabla^2 W + \varepsilon \dot{W}(x,y,t) + \varepsilon^2 . p'(x,y) \tag{10}$$

We now replace the first two terms in the right member of (7) by their blurred derivatives counterparts. For the first one we use the third generation zero order kernel (6).

$$W(x,y,t+\varepsilon) \equiv \int \left({}^3P^0_{(\mathbf{r}'-\mathbf{r},\delta)} - \varepsilon^2 \kappa P^4_{(\mathbf{r}'-\mathbf{r},\delta)} \right) W(\bar{x},\bar{y},t) d\bar{V} + \varepsilon \dot{W}(x,y,t) + \varepsilon^2 . p'(x,y) \tag{11}$$

Finally, we relate the time step ε to the parameter δ of the blurred derivative through

$$\varepsilon^2 \kappa = \frac{\delta^4}{32} \tag{12}$$

Hence, using relation (7) we have:

$$W(x,y,t+\varepsilon) \cong \int P_{(\mathbf{r}'-\mathbf{r},\varepsilon)} W(\bar{x},\bar{y},t) d\bar{V} + \varepsilon \dot{W}(x,y,t) + \varepsilon^2 . p'(x,y) \tag{13}$$

The operator $P_{(\mathbf{r}'-\mathbf{r},\varepsilon)}$ is termed infinitesimal propagator because its effect on the field W(x,y,t) is to propagate it in time an infinitesimal amount ε.

4 COMPUTATIONAL IMPLEMENTATION

To obtain a numerical scheme from equation (13) the domain of interested is filled with nodes, not necessarily equally spaced, and the unknown field W(x,y) is approximated by a prescribed function around each node. The simplest function is a *local* fourth degree polynomial whose coefficients relate the unknown at the current node with its value on some number, M, of neighboring nodes. Hence, calling $\tilde{W}$ the local approximation we have:

$$\tilde{W}_{(x,y)} = \mathbf{a}.\mathbf{R}_{(x,y)} \tag{14}$$

where

$$\mathbf{R}_{(x,y)} = (1, x, y, x^2, xy, y^2, x^3, x^2 y, ..., y^4)^t \;\; ; \;\; \mathbf{a} = \begin{bmatrix} a_1 & a_2 & a_3 & a_4 & a_5 & a_6 ... a_{15} \end{bmatrix}^t \tag{15}$$

The vector of coefficients **a** can be calculated in terms of the M nodal values of **u** solving[14]:

$$\mathbf{a} = (\mathbf{V}^t.\mathbf{V})^{-1}.\mathbf{V}^t.\mathbf{u} \tag{16}$$

where

$$\mathbf{u} = \begin{pmatrix} u_0 & u_1 & \cdot & \cdot & u_M \end{pmatrix}^t \quad ; \quad \mathbf{V} = \begin{bmatrix} 1 & x_0 & y_0 & x_0^2 & x_0 y_0 & y_0^2 & \cdot & \cdot & y_0^4 \\ 1 & x_1 & y_1 & x_1^2 & x_1 y_1 & y_1^2 & \cdot & \cdot & y_1^4 \\ \cdot & & & & & \cdot & \cdot & \cdot & \cdot \\ \cdot & & & & & \cdot & \cdot & \cdot & \cdot \\ 1 & x_M & y_M & x_M^2 & x_M y_M & y_M^2 & \cdot & \cdot & y_M^4 \end{bmatrix} \tag{17}$$

The matrix $\mathbf{V}^t.\mathbf{V}$ of a least square fit – eq. (16) – is known to be very poorly conditioned, specially when the degree of the polynomial is high. This may lead to substantial numerical error which pollutes the solution. Hence, a better alternative is to directly compute the pseudo-inverse of matrix $\mathbf{V}$ using singular value decomposition.

To obtain a numerical scheme discretization (14) is fed into the updating prescription (13). In the case of equilibrium the state does not evolve and velocities are zero so that the discrete equation of a given interior node "i" takes the form:

$$W_i \cong \int P_{(\mathbf{r}'-\mathbf{r},\varepsilon)} \widetilde{W}(\overline{x},\overline{y}) d\overline{V} + \varepsilon^2 . p'(x,y) \tag{18}$$

Where $\widetilde{W}$ is the local polynomial approximation (15 – 17) around node "i" in terms of its (M-1) neighbors.

To model free vibrations we proceed as usual assuming that displacements vary harmonically:

$$\begin{aligned} W(x,y,t) &= W(x,y)e^{i\omega t} \quad ; \quad \dot{W}(x,y,t) = i\omega W(x,y)e^{i\omega t} \\ W(x,y,t+\varepsilon) &= e^{i\omega\varepsilon} W(x,y)e^{i\omega t} \end{aligned} \tag{19}$$

Replacing relation (19) in equation (13) an eigenvalue equation is obtained:

$$\int P_{(\mathbf{r}'-\mathbf{r},\varepsilon)} \widetilde{W}(\overline{x},\overline{y}) d\overline{V} + \lambda\, W(x,y) = 0 \tag{20}$$

Where $\lambda = i\omega\varepsilon - e^{i\omega\varepsilon}$

As regards boundary conditions, it is necessary to enforce two data at each point. One of them is the local displacement, W_0 , and the other is either the local curvature parallel to the outward normal, $\partial W / \partial n$, or the corresponding bending moment, M_n . In methods based on weak formulations this is achieved by defining three fields at each node: displacement and its two partial derivatives. The present method, however, used only one variable per internal node (the displacement) so that a different procedure should be used. We resorted to a very simple and effective one which is to just place two nodes at each boundary point, carrying the corresponding pair of local boundary data. The treatment of the local prescribed displacement is trivial and similar to the finite element procedure. The other node however requires to

modify its contribution to the Vandermonde matrix (17) of any node linked to it. Let us assume for instance that the prescribed value is the first derivative $\partial W/\partial n$, where the outward normal is $\hat{\mathbf{n}} = (n_x, n_y)^t$. Hence, this boundary node is the k-th node in the cloud of a given interior node the corresponding row of (17) must be replaced by the derivative of the polynomial (15):

$$\frac{\partial \mathbf{R}}{\partial n} = \frac{\partial \mathbf{R}}{\partial x} n_x + \frac{\partial \mathbf{R}}{\partial y} n_y = (0, n_x, n_y, 2x_k n_x, y_k n_x + x_k n_y, 2y_k n_y, ..., 4y_k^3 n_y) \tag{21}$$

Similarly, if the prescribed value is a bending moment $M_n = \frac{\partial W}{\partial n} + \nu \frac{\partial W}{\partial b}$ (where $\hat{\mathbf{b}} = (n_y, -n_x)^t$ is the local tangent to the boundary) the corresponding derivative of $\mathbf{R}$ should be used:

$$\mathbf{R} \rightarrow \frac{\partial \mathbf{R}}{\partial n} + \nu \frac{\partial \mathbf{R}}{\partial b} \tag{22}$$

5 NUMERICAL RESULTS

To test the performance of the technique we modeled a simply supported square plate of side a=20 mm and thickness h=0.5 mm with a uniformly distributed load p=10 Mpa. The analytical solution for this problem has the form of a Fourier series:

The material has a Young modulus E=140000 Mpa and Poisson ratio $\nu = 0.3$. We used nine different meshes of equally spaced points ranging from 9X9 to 25X25. The polynomial approximation of the present method has 15 coefficients. Hence, for each interior point we used the 24 first and second neighbors forming a square. The problem was also solved using square finite elements. In this case each interior node is connected to first eight neighbors forming a square. However, in this case each node has three degrees of freedom (transverse displacement and its two first derivatives). As a consequence, in FIM each row of the stiffness matrix has 25 non-zero entries while in finite elements it has 27. But the matrix of FIM is non-symmetric so that the computational cost is somewhat higher but of the same order.

Figure 1 shows error versus nodal distance h in logarithmic scale for FIM and FEM. It can be seen that the error with FIM is always lower that with FEM. Also, the convergence rate with the latter is two, as predicted by theory, while with FIM it is three. Hence, at the expense of a slightly higher computer cost (due to non-symmetry) FIM provides a substantially enhanced convergence rate.

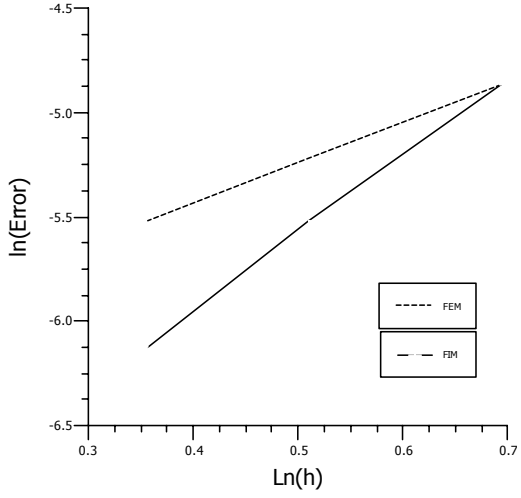

Figure 1: Convergence of FEM and FIM for regular meshes.

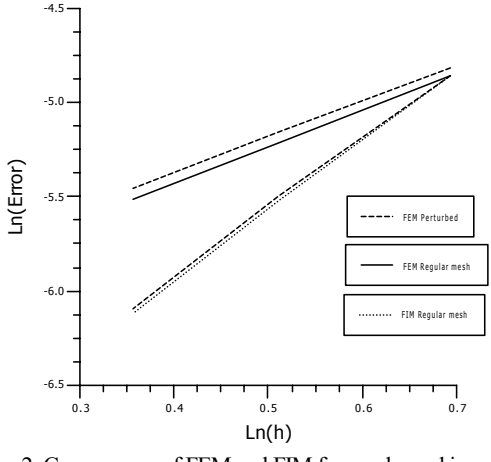

Figure 2: Convergence of FEM and FIM for regular and irregular meshes.

In order to compare the performance of both schemes for irregular arrays of nodes (where a meshless method is supposed to offer an advantage over FEM), we solved the same problem but moving all interior nodes at random a distance of ten percent the nodal spacing. Results are shown in Figure 2. While FEM results are now much less accurate than with a regular net of nodes, the error with FIM is only marginally increased. Moreover, the convergence rates of both schemes are the same as in Figure 1. Hence, the meshless scheme is expected to be advantageous for irregularly shaped plates.

Finally, we calculated eigenfrequencies of the same plate with all boundaries clamped. The analytical solution is:

$$\omega_{mn} = h\sqrt{\frac{E}{12\rho(1-\nu^2)}}\frac{(m^2+n^2)}{a^2} \quad ; \quad m,n = 1,2,3,.... \tag{23}$$

For the numerical simulations we used a mesh of 11X11 nodes. Comparison of exact and numerical results for the first three modes are shown in table 1. In this case both numerical methods provide very similar results, with FIM slightly in excess of exact values.

m	n	Exact	FEM	FIM
1	1	147.8	147.7	148
1	2	369.5	369.3	369.7
2	2	591.2	590.4	591

Table 1: First three frequencies for free vibrations of square plate.

6 CONCLUSIONS

An extension of the Functional Integral Method for solving Kirchhoff plate model problems is presented. The implementation used local fourth order polynomial interpolation using the first 24 neighbors for each internal node. To account for boundary conditions two nodes are placed at each point of the boundary: one of them carries the prescribed displacement and the other one the prescribed derivative (either first derivative of displacement or bending moment). The numerical scheme has been compared with quadrilateral plate finite elements, which used the first eight neighbors for each internal node. Numerical results for static test problems indicate that the present method not only achieves better accuracy than FEM when the same nodes are used, but also that the rate of convergence is substantially higher. In particular, FIM has shown to be less sensitive to irregularity of the net of nodes so that it is specially suited to

model highly irregular domains. For free vibrations of plates on the other hand both methods perform similarly. Hence, the proposed method is a viable alternative for modeling of plates.

7 REFERENCES

[1] Nayroles B., Touzot G, Villon P., Generalizing the finite element method: diffuse approximation and diffuse elements. *Computational Mechanics*, 1992; **10**: 307-318.
[2] Belytschko T., Krongauz Y., Organ D., Fleming M., Krysl P. Meshless methods: an overview and recent developments. *Computer Methods in Applied Mechanics and Engineering* 1996; **139**: 3-47.
[3] C.A Duarte and J.T. Oden, `H-p adaptive method using clouds', *Comput. Methods Appl. Mech. Engrg*., **139**, 237-262 (1996).
[4] J.J. Monaghan, `An introduction to SPH', *Computer Physics Communications*, **48**, 89-96, (1988).
[5] W.K. Liu, S. Jun and Y.F. Zhang, `Reproducing Kernel Particle Methods' , *Int. J. Numer. Meth. Engng*, **20**, 1081-1106 (1995)
[6] N. Sukumar, B. Moran and T. Belytschko, `The Natural Element Method in Solid Mechanics' , *Int. J. Numer. Meth. Engng*, **43**, 839-887 (1998).
[7] T. Liszka, 'An Interpolation Method for an Irregular Net of Nodes', *Int. J. Numer. Methods Engng*, **20**, 1599-1612 (1984).
[8] C.S. de Barcellos, P.T.R. Mendonca, and C.A. Duarte, "Investigation of Timoshenko beam problems using hp-Cloud meshless FEM", Computational Mechanics: new trends and applications, Barcelona, Spain, (1998).
[9] O. Garcia, E.A. Fancello, C.S. de Barcellos, and C.A. Duarte, "hp-Clouds in Mindlins thick plate model", Computational Mechanics: new trends and applications, Barcelona, Spain, (1998).
[10] J. Sladek, V. Sladek and H.A. Mang, "Mehsless formulation for simply supported and clamped plate problems", *Int. J. Num. Meth. Engng,* **55**, 359-375 (2002)
[11] E. Pardo, "Meshless method for linear elastostatics based on a path integral formulation", Int. J. numer. Methods Engng., 47, 1463-1480, (2000).
[12] E. Pardo, "Convergence and accuracy of the path integral approach for elastostatics", Com. Methods Appl. Mech. Engng., **191 (20)**, 2219-2247 (2002).
[13] E. Pardo, "Functional integral formulation of classical wave equations", J. Sound and Vibr. (in press).
[14] P. Lancaster and K. Salkauskas, *Curve and Surface Fitting*, Academic Press, 1986.